Experimental processing of physical model data from circular arrays

David C. Henley
CREWES, Dept of Geoscience, University of Calgary

Summary

Many transducer configurations can be used for probing and imaging targets in a physical modeling tank. We describe experimental processing used to extract target information from a physical model where the transducer geometry consists of a circular array of discrete receivers surrounding a target of unknown shape and location, with sources positioned regularly on the circumference of the same circle as the receivers. Each source ensemble consists of recorded signals from all the receivers on the circular array accessible from that source, subject to the mechanical positioning limitations of the modeling system. The modeling and processing experiment described here attempts to extract the 2-D shape and position of an object enclosed by the circular array, using concepts of projection. Target information in this experiment consists of variations of first-arrival wavelet amplitudes and transit times from those measured by the same circular array in an empty, uniform medium. Hence our processing efforts are aimed at detecting those variations, projecting them as "shadows", and combining the shadows from the processed source gathers to form a crude image of the target, for use as the starting point in an FWI procedure.

Method

Physical modeling can be used to study a variety of problems where measurements of acoustic or elastic waves are used to obtain basic information about the object or target being investigated. The current physical modeling system developed and operated by CREWES has been used in many studies of elastic wave propagation suggested by various projects in the real world of seismic exploration, as well as those in wave propagation theory (Wong et al, 2016, Romahn and Innanen, 2017, Wong et al, 2019, Henley and Wong, 2019, Henley, 2020). In the present study, we exchange the environment of seismic exploration for that of medical imaging, with the hope that methods developed for seismic imaging can be used to enhance images used for medical diagnosis.

The use of ultrasound to probe the human body and provide images of internal human organs is widespread; and has played a key role in the early diagnosis of many illnesses (Henley, 2021). Conventional ultrasound diagnosis uses a coincident source and receiver, which is applied to various locations on the surface of the body to form images of structures within the body. Because most body tissues are very absorptive and don't differ much in elastic properties, the resulting images are sometimes faint and difficult to interpret. What we demonstrate here is a different mode of imaging, in which an ultrasonic source radiates its energy into many receivers at different directions and distances from the source, using an arrangement similar to that used for X-rays in a CT scan. In such a survey, we obtain backscattered events that can contribute directly to an image, as well as transmitted signals that can lead to tomographic images of transit time ('time of

flight'), or material absorption. Here, we focus on using transmitted first arrival events to create a first estimate of an image for use in FWI procedures.

The experimental geometry

The experimental setup consists of a circular array (scaled radius 1500m) of 72 discrete positions where an ultrasonic piezopin transducer can be positioned in water in our modeling tank to act as a receiver. On the same circle are located 36 source positions where a second piezopin transducer can be located to act as a source. Ideally, we fire the source into the receiver at each of its 72 possible positions, for each unique source position, to provide a source ensemble consisting of 72 traces for each of the source positions. Practically, however, the transducer positioning fixtures must be prevented from colliding, which limits the accessible receiver positions for many sources. Instead of the 2592 traces we would expect for fully accessible array positions, in practice, we obtain only 1331. Figure 1 shows the basic layout of the circle acquisition geometry.
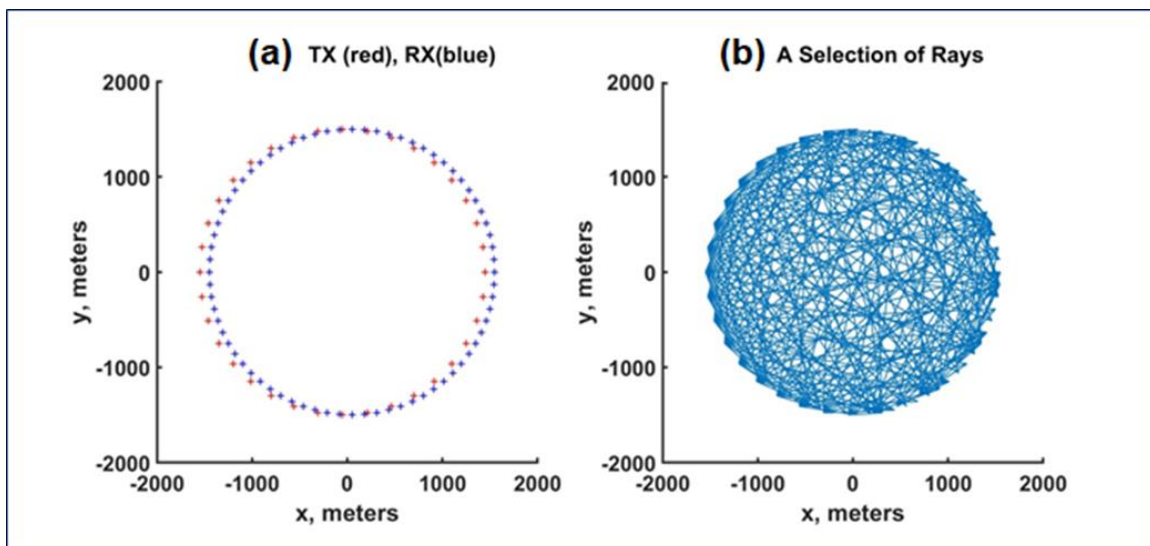

FIG. 1. (a) Schematic of acquisition geometry used for simulating the 1500m scaled radius physical model experiments. Note that there are 36 source positions (red), but twice as many receiver positions (blue), and that source and receiver can never be collocated due to the mechanical limitations of the acquisition apparatus. (b) A selection of possible raypaths along which acoustic energy can be transmitted. Not all these raypaths can be realized due to physical interference limitations of the acquisition apparatus. (Figure courtesy of Joe Wong).

Using this experimental setup, we conducted two basic experiments; the 'null' experiment, where we recorded a full suite of source gathers in unobstructed pure water, and the 'target' experiment, in which we placed an object in the water somewhere inside the circumference of the acquisition circle and acquired a another full suite of source gathers, which contained information about the intruding object. We then analyzed the 'target' survey alone, and, as well, subtracted the processed waveforms of the two surveys to explore the 'difference' image. Here, we describe our processing efforts on the 'target' survey only

'Conventional' processing

Our goal in this first step of data analysis is to examine first arrival events, so we first applied steps to reduce the size of the data set and to make these events easier to examine visually. Since the background medium of the model is water, we first computed all the source-receiver offset values from the known x and y acquisition coordinates, then computed the transit time between each pair of source and receiver positions. These transit time values were stored in trace headers as 'vel_stat', a static shift corresponding to the source-receiver time separation in water. When vel_stat is applied to each trace as a static shift, the first arrival waveforms become approximately aligned, which allows the traces themselves to be truncated for display (we chose 500ms, and appended 100ms of blank trace ahead of the arrival waveforms to make them easier to examine). To remove jitter in the arrivals we applied a trim statics technique, with an aperture equal to the total number of traces in the data set. The traces in each gather are ordered by source-receiver azimuth, and hence correspond to a 'fan' of raypaths from the source position to all receivers accessible from this source point. We applied Gabor deconvolution and bandlimiting to shape arrival wavelets, and spherical spreading correction, to adjust amplitudes for the different path-lengths for the traces spanning the circular array.

Figure 2a shows a group of raw source gathers of traces recorded with the described experimental setup for the 1500m circular array, with a PVC target placed somewhere inside the circular array. We observe that the arrivals for the most direct raypaths can easily be seen, although some of them seem to be missing or highly attenuated (arrows) due to the presence of the target. Figure 2b shows the same source gathers after water-transit correction, trim statics, wavelet shaping, and spherical spreading correction. On these gathers, it becomes clear that the actual first arrivals within the 'dim' spots on the original gathers in Figure 2a occur at earlier transit times than predicted by water transit time, indicating their passage through a material whose velocity is greater than that of water. Arrivals near the edges of these dim spots are somewhat confused, likely indicating diffraction around the object (arrows). Figure 2b shows a picked horizon which includes these shallow first arrivals and can be used to 'flatten' the gathers.
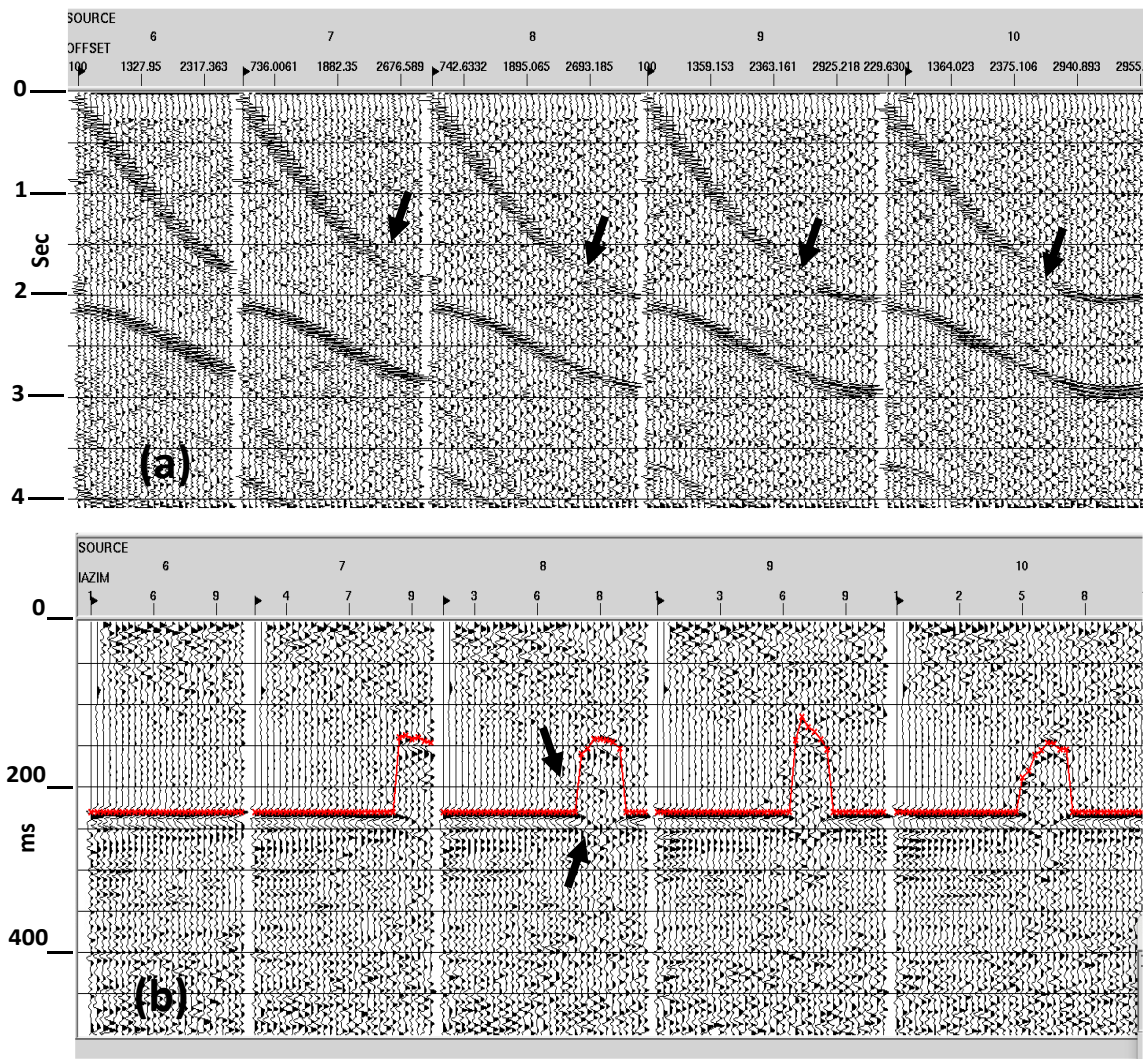
FIG. 2. a) Five recorded source gathers from the 1500m circle experiment with a PVC target present inside the circular array. The presence of the target is revealed by the zones of attenuated direct arrival amplitudes for source numbers 7-10 (arrows). b) The same source gathers as in Figure 2a, but with all preliminary processing applied, and first arrivals picked in the anomalous regions. Note the diffraction-like events at the edges of the anomalies.

'Novel' Processing

Next, we experimented with some 'creative' processing techniques, in which we altered the coordinates of the recorded data according to strictly 'geometric' considerations, to allow us to apply simple array transformations to the data, which enable us to combine the modified data gathers into 'shadow images' showing the rough location and shape of the target object.

To this point, we have displayed the data amplitudes using coordinates of transit time, and either source-receiver offset, or source-receiver azimuth. We next assigned arbitrary coordinates to the data amplitudes; in particular, substituting various trial formulae for computing 'source-receiver offset' for the horizontal coordinate. The values assigned may have little or no relation to actual offset, but simply define the secondary coordinate of a particular data ensemble to enable us to adapt existing seismic data operations to remap the data matrix sample values geometrically.

Forming the object shadows in the source gathers.

Our goal for this stage of processing was to create projected 'shadows' of the target object in each source gather and transform the gathers for stacking, to create a 'shadow image' of the target relative to the circular array. First, we applied a non-linear process to create shadows in the source gathers:

- We picked the anomalous arrivals seen on all source gathers, as in Figure 2b, and applied the picks as a horizon for flattening all the source ensembles to a common arrival time. The flattening operation shifts the anomalous traces and alters their 'end of live samples' trace header.

- We checked the 'end of live samples' trace header for each trace. Any trace whose 'end of live samples' header exceeds the nominal value was flagged as a 'shadow' trace.

- All trace sample values in each gather were zeroed outside the shadow, and were set to unity inside the shadow, to create 'black' shadows.

Manipulating the object shadows

We used two simple re-mapping operations that can be applied to 2D seismic trace panels to rotate their sample values to new coordinates; the Radial Trace Transform (Henley, 1999a, and Henley, 2011) and the Linear Moveout correction. Both require the signed source-receiver offset trace header; but we can define this header any way we like, to create the geometrical relationship desired. For both operations, we ignore their original purpose, and use the offset header value as a parameter to re-map data arrays.

In the case of the Radial Trace Transform, amplitudes are re-mapped from the original domain of primary trace coordinate and transit time to a new domain of ray parameter and transit time. The sampling trajectory slope can be chosen to isolate a single predominant slope (RT dip transform, Henley, 1999b). In this application, we chose the RT dip transform with the dip slope velocity as a user parameter to be chosen in conjunction with the 'offset' trace headers placed in the source gathers.

The Linear Moveout operation applies time shifts to seismic traces that are proportional to the 'offset' header in each trace, with the velocity parameter in the LMO operation determining the trace shift relative to its posted offset value. The earlier RT transform destroys the original offset values in the trace headers, so we can create any set of headers that will help orient the shadows during the LMO. After some experimentation, we determined that an offset formula with increment

based on the trace sequence number within a source gather, scaled by the sum of the source-receiver azimuth and the azimuth of the source from the circular array centre, can be adjusted to approximately provide the desired angular rotation of each shadow within its 2D source array.

Figure 3a shows the projected unitary RT domain shadows for sources 15-21 after rotation and shift operations via the Linear Moveout operation using trial parameters. Figure 3b is the resulting trial stack of similar shadows from all sources. Dimensions for the image in 3b are not shown because of computational uncertainty (research in progress), but both are spatial coordinates.
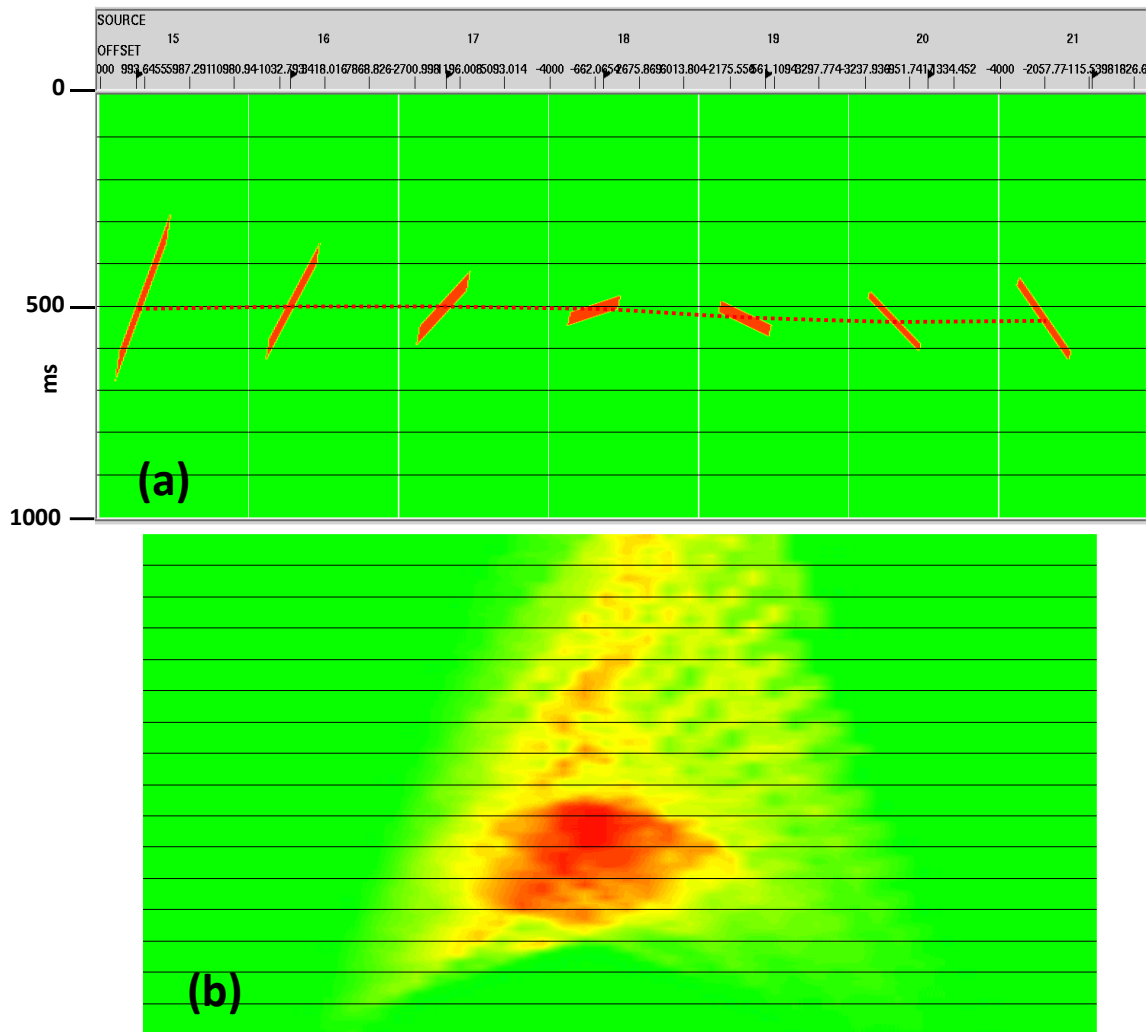

FIG. 3 a) Shadows created for source gathers 15-21, after RT Transform and LMO. b) Trial stack of all shadows from experimental processing—dimensions undefined.

Conclusions

We have shown an attempt to use transmission acoustic arrivals acquired using a circular array of ultrasonic transducers to provide an estimate of the shape and location of a solid target immersed in water within the array. While the arithmetic details of the actual transformations remain uncertain, we have shown the feasibility of the proposed method by using trial parameters to create a suite of projection shadows that, when stacked, provide a reasonable image of the target object, albeit without necessary physical dimension information at this stage. In addition to clarifying the necessary trace header arithmetic, ongoing research will investigate creation of 'grey' shadows with varying density to replace the current 'black' shadows.

Acknowledgements

References

Henley, D.C., 1999a, Coherent noise attenuation in the radial trace domain: introduction and demonstration: CREWES Research Report, **11**, 36, 37.

Henley, D.C., 1999b, Demonstration of radial trace domain filtering on the Shaganappi 1998 2-D geotechnical survey: *CREWES Research Report*, **11**, 58, 17.

Henley, D.C., 2011, Now you see it, now you don't: radial trace filtering tutorial: CREWES Research Report, **23**, 44, 25.

Henley, D. C., and Wong, J., 2019, Let there be light: illuminating physical models from the surface: *CREWES Research Report*, **31**, 22, 27.

Henley, D. C., 2020, A tale of two realities; reconciling physical and numerical modeling via 'bootstrap' processing: *CREWES Research Report*, **32**, 23, 28.

Henley, D.C., 2021, Personal note: In July 2021, the experienced analysis of an abdominal ultrasound session by an alert physician at the imaging laboratory sent me to the ER for emergency gallbladder surgery and other procedures, that likely prevented me from experiencing rather serious consequences.

Romahn, S. J., and Innanen, K. A. H., 2017, The seismic physical modelling laboratory as a tool for design and appraisal of FWI methods: *CREWES Research Report*, **29**, 66, 22.

Wong, J., Bertram, K. L., and Hall, K. W., 2016, Physically-modeled 3D surveys over a channel structure: CREWES Research Report, **28**, 79, 8.

Wong, J., Zhang, H., Kazemi, N., Bertram, K. L., Innanen, K. A. H., and Shor, R., 2019, Physical modeling of seismic illumination and SWD: CREWES Research Report, **31**, 53, 14.